Development of an optical read-out for GEM detector stability studies

Bachelor Thesis

Berkin Ulukutlu

24.09.2018

Supervisor:
Dr. Piotr Gasik
Dense and Strange Hadronic Matter Group
Physik-Department E62
Technische Universität München
p.gasik@tum.de

Primary reviewer: Prof. Dr. Reinhard Kienberger
Secondary reviewer: Prof. Dr. Laura Fabbietti

ABSTRACT:

This thesis summarizes the research and work done in GEM detector stability studies. GEMs type of detectors are among gaseous ionization detectors that offer many advantages such as ion back-flow mitigation over more traditional detector architectures like MWPCs. However, the operation of GEMs is limited by the fact that GEMs are fragile against electrical discharges. For this reason, the stability of the detector against discharges is a crucial performance indicator for GEMs. Throughout this thesis two major tasks are undertaken. Firstly, a comprehensive discharge stability study on a type of GEM detector called THGEMs is conducted. The discharge probability of the THGEM (the measure indicating the stability of the detector) is measured using four gas mixtures and compared to previous results of standard GEMs. The THGEM displayed higher discharge probability of upto two orders of magnitude for a given gain setting. A possible reason for this worse performance of THGEMs and the underlying mechanisms of discharge formation is discussed. Secondly, the development of an optical read-out system for secondary discharge studies is introduced. Secondary discharges are events where the initial discharge propagates inside the detector chamber possibly harming the equipment critically. The physical mechanism behind this propagation is not yet understood and new methods for probing this phenomenon are important. The developed optical read-out system aims to capture very precise images of these events as a new tool of studying them. The imaging system was implemented and commissioned by capturing tracks of alpha particles. It yielded great results in terms of needed image resolution and high low-light sensitivity for the proposed study on discharge propagation.

With my signature below, I assert that the work in this report

"Development of an optical read-out for GEM detector stability studies"

been composed by myself independently and no source materials or aids other than those mentioned in the report have been used.

I agree to the further use of my work and its results for research and instructional purposes.

I have not previously submitted this thesis for academic credit.

Place, Date	Signature

Contents

1 Introduction **6**
1.1 Gas Electron Multipliers 6
1.2 Discharges and propagation 8

2 THGEM Stability Studies **10**
2.1 The setup 11
2.2 The measurement methods 13
2.3 Results 14

3 Optical Read-Out System **19**
3.1 Design and production of the optical read-out system 20
3.2 Alpha particle tracking 25

4 Summary and Outlook **30**

5 Acknowledgements **31**

List of Figures

1 Working principle of GEM detectors 6
2 Visualisation of field lines in GEM holes and GEM hole photo [1] 7
3 Picture of a malfunctioning GEM after a discharge occurence [2]. 8
4 The 3x3 cm^2 THGEM foil from INFN Trieste 11
5 The emission spectrum of the mixed alpha source [3] 11
6 Schematic of the THGEM Detector 12
7 Pictures of the THGEM Detector 12
8 Gain measurements for THGEM with four different gas mixtures 14
9 An example current measurement with discharges 15
10 Gain measurement for Ar-CH_4 with and without discharge filtration 16
11 Discharge probability measurements for THGEM with four different gas mixtures 17
12 THGEM discharge probability compared to the values obtained with standard GEMs (from [4]). 18
13 Schematic of the used GEM detector configuration 20
14 Secondary scintillation spectrum of Ar-CF_4 (80-20) [5] 21
15 The technical drawing of the camera housing 22
16 The detector with the camera housing 23
17 Andor Zyla 5.5 camera 24
18 Diagram of the optical readout setup 25
19 Images of alpha tracks captured with the optical read-out 26
20 Two alpha traks captured in the same exposure 27
21 Alpha tracks with scattering event 27
22 Bragg peak like profile over the track line 28
23 The emissions of a second alpha particle during the decay of ^{216}Po to ^{212}Pb 29
24 Decay chain of ^{220}Rn [6] 29

1 Introduction

1.1 Gas Electron Multipliers

GEM (Gas Electron Multiplier) detectors are a type of gaseous ionization detectors used in particle physics experiments for detecting ionizing particles [1]. The production and operation methods of GEMs have been extensively studied and improved since its invention by Fabio Sauli in 1997 at CERN [7, 8]. GEMs in comparison to more traditional gaseous detectors such as MWPCs (Multi-wire Proportional Chamber) offer advantages like intrinsic suppression of the ion-backflow and allowing much more flexibility in the designing of its geometry [9].

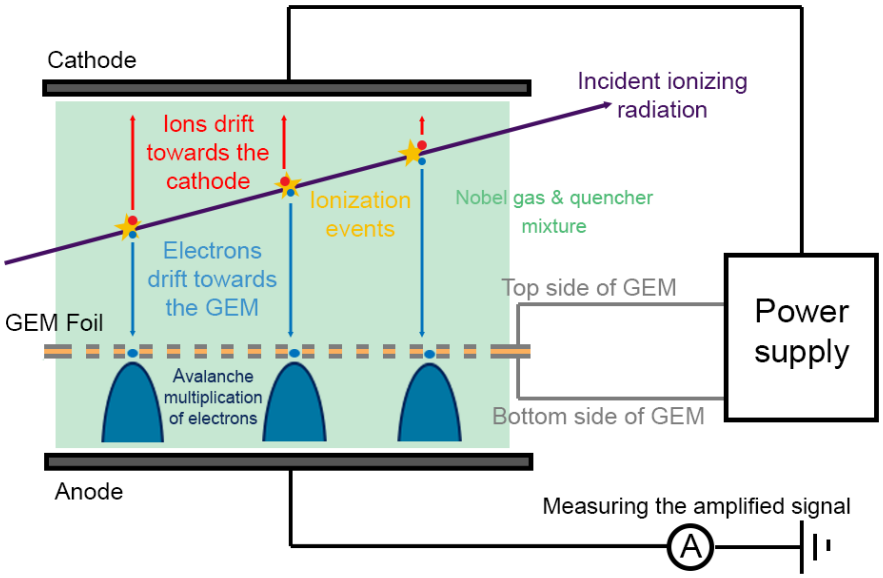

Figure 1: Working principle of GEM detectors

A diagram showing the basic working principle of GEMs is given in figure 1. The incident ionizing particle to be detected enters the detector filled with a strictly regulated mixture of noble gas and quencher. The particle ionizes the gas molecules on its trajectory as it interacts with the surrounding medium. Through the ionization events electron-ion pairs are created. These pairs, which would recombine under normal circumstances, are separated by the applied ambient electrical field called the drift field. The electrons drift towards the GEM foil whereas the oppositely charged ions drift towards the cathode. The very thin GEM foil is usually made of a polyimide sheet (thickness of 50 μm) with copper clads on both its sides. The foil has multiple tiny holes (diameter of 50 μm) on its surface where the drifting ionisation electrons enter. The applied potential difference to the electrically separated top and bottom sides of the foil results in a very concentrated electric field within the GEM holes hence the geometry. With this electrical field, the electrons accelerate as they pass through the GEM holes and ionize more atoms and molecules.

The newly liberated electrons repeat the process resulting in the Townsend avalanche multiplication phenomenon of charges [10, 11]. The increased quantity of electrons exiting the holes drift toward the anode, where they recombine and produce a current signal. Finally, this current signal from the anode (often segmented in design to be able to produce two dimensional tracks of the incident particle) is measured with read-out electronics [12].

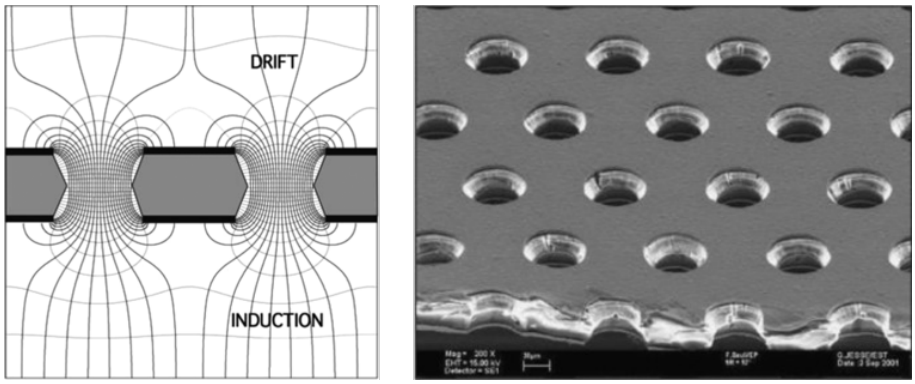

Figure 2: Visualisation of field lines in GEM holes and GEM hole photo [1]

The GEM detectors can thus amplify the signal from even a single ionisation event to measurable levels. The measure for this amplification is dubbed gain and it depends exponentially on the applied voltage across the GEM foil. The gain is also affected by the used gas mixture, foil type and detector geometry. For example, stacking of multiple GEM foils operating the detector with very high gains is possible. Furthermore, another important aspect of GEMs geometry is that the positively charged ions created during the avalanche process end up on the top side of the foils[7]. With multi-wire proportional chambers the ions drift all the way back to the cathode electrodes and create inhomogeneities in the drift field. The common way to minimise the number of back-drifting ions is to use a so-called "gating grid" which, in turn, limits the maximum rate of MWPCs [13]. Since GEMs suppress the ion-backflow, this relatively new type of detector is being implemented more commonly as collider experiments reach higher rates [14].

1.2 Discharges and propagation

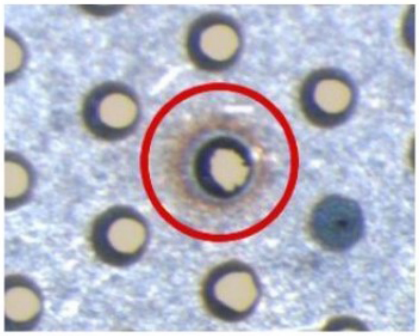

Figure 3: Picture of a malfunctioning GEM after a discharge occurence [2].

During the operation of a GEM detector with high gain it is possible that electrical discharges occur. Discharges are break down events where the gas in the detector momentarily conducts relatively high currents depositing energy in forms of light, heat and sound. Because of the very small sizes concerning its components, GEMs are prone to get critically damaged by these events. Discharge events affects the detector in many ways. The potential difference between the two sides of the foil drops after a discharge rendering the GEM momentarily blind until the power supply restores the potential levels. On rarer instances the GEM foil in the detector might even get shorted as the heat from the discharge melts the material in one of its holes requiring the replacing of the foil. An example of such damage is shown in figure 3. Some material deposits caused by the discharge can be seen inside the marked hole. [15] The electronic read-out system connected to the anode might also get damaged if the discharge propagates to the anode. With all these reasons, avoiding discharges is very crucial for GEM operation and has been a topic of great interest and research throughout the years [16, 17, 18].

There are two types of discharge events to occur in GEMs. These are called primary and secondary (propagated) discharges. The physics of the formation of primary discharge events is understood and well-studied [19]. It relates to the Raether limit in proportional chambers, where if the space charge created from the avalanche charge multiplication exceeds a certain amount (Qmax = 10^8e), it effects the electric field so much that the avalanche transits into a streamer. The streamer can expand and may form a conductive link between the two potential levels creating a spark [20]. A similar charge limit was found for GEMs; where if the accumulated charges in a GEM hole exceed a certain threshold (Qcrit = $(5-9)10^6$e) discharges occur [4]. This threshold is observed to be dependent on the used gas mixture and on the geometry of the used GEM foil.

The primary discharges occurring inside the holes have also been observed to propagate to the gap between the foil and the anode electrode (or to the foil underneath if in stack). [17] These propagated discharges are termed secondary discharges and they involve much higher energy depositions and are generally much more harmful to the detector. Although there has been an extensive search regarding this topic, the physics of this propagation mechanism is however not yet fully understood. There are some proposed mechanisms un-

der consideration. These include: Deposition of conductive material into the gap after the initial discharge or the high temperature wave created by the primary discharge leading to thermal ionization in the relatively weak field in the gap and many more. Furthermore, some UV-light based mechanisms like photoionization have been ruled out since the secondary discharge has been observed not to occur immediately after the initial discharge but after a delay (∼10-6 s). To further our understanding of this subject many studies of simulating the discharges have been conducted. Also, there are new methods for probing discharge propagation such as using optical read-out which are planned to bring new viewing angles on this phenomenon.

There have also been many breakthroughs regarding mitigating discharges in GEMs. For example, implementing multiple foils in a stack configuration has been shown to increase the stability of the detectors against discharges [17]. The underlying mechanism for this is that the diffusion of the stream of electrons as it transverses the gap in between the consequent foils. The total charge leaving a hole in the upper foil spreads over multiple holes in the next foil. Because of this, with each consecutive layer the total gain achieved in the foil can increase without exceeding the Raether limit like threshold of each individual hole. With this it has been shown that using stacks of GEM foil can reduce the overall discharge probability of the detector whilst maintaining the gain level, and this architecture is thus very widely implemented. Other than this adding protective decoupling resistors to the foils and segmenting the read-out electrodes are also used extensively to lessen the risk of damaging the detector with discharges [16].

It is also worth to note that since the invention of gas detectors the knowledge on the topic of discharges has shown a rapid increase. The relatively small scale and simple geometries of these detectors represent probably the simplest physics case for this very complicated phenomenon [21]. In the following chapters studies and the development of new methods on the stability of GEM detectors against discharges will be discussed. Firstly, a conducted stability analysis on a THGEM is introduced in chapter 2. THGEMs are a type of GEM detectors and offer a good alternative to the standard GEMs with their more robust and easy to handle design. However their performance in terms of stability against discharges was previously not comprehensively investigated. The used setup, measurement methods and the obtained results are discussed . Secondly, the development of a new optical read-out system for a GEM detector is introduced in chapter 3. The development of the setup includes the building of the modified detector chamber and camera housing, optimisation of the process of operating the used scientific camera and the initial testing of the system by capturing tracks of alpha particles. The developed read-out system is planned to be used to acquire images of secondary discharges, a discharge propagation phenomenon that is still not fully understood.

2 THGEM Stability Studies

GEM detectors come in a multitude of different setups and configurations. Many of the parameters in the design of the detector, like foil type, foil number and distances between subsequent GEMs influence its performance in terms of gain and stability against electrical discharges. Even since GEM technology has been known for more then twenty years, new designs are still being developed, tested and optimized for various experimental uses.

One of the earlier developed configurations include THGEM (Thick GEM) foils instead of standard GEM foils introduced in section 1. The name comes from the fact that THGEMs, in comparison to normal GEMs, are much thicker. The dimensions of THGEMs are usually close to an order of magnitude larger then with standard GEMs, including the hole diameters. These holes can be mechanically drilled into a Printed Circuit Board (PCB) making the production process much simpler. THGEMs are much sturdier and usually easier to handle because of their thicker form. Furthermore, they are more durable against dust and other factors like discharges, which can damage normal GEMs irreparably. With these reasons THGEM foils offer a good alternative to normal GEM foils for setups where the operating conditions might be more hazardous.

Considering this, it is important to have comprehensive results on THGEMs performance in terms of gain and discharge stability. So far, there are no dedicated and comprehensive studies on THGEM stability against electrical discharges. In this work, the systematic study of sparking probability in different gas mixtures is presented. They were conducted in parallel to the construction of the optical read-out, which will be further discussed later. [see chapter 3]

2.1 The setup

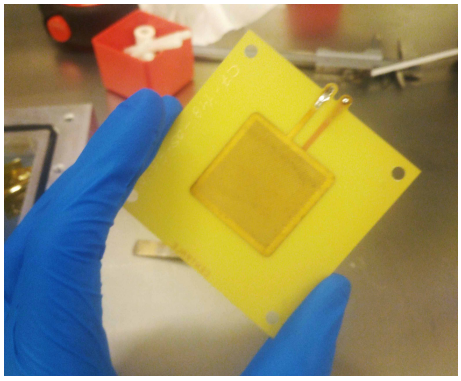

Figure 4: The 3x3 cm^2 THGEM foil from INFN Trieste

The THGEM foil used in the studies has an active area of 3x3 cm^2 and a thickness of 0.4 mm. The holes on the foil have a diameter of 0.4 mm and a pitch of 0.8 mm. The main body of the foil is composed of PCB material with copper clads on both sides acting as the top and bottom electrodes.

The foil is installed inside the detector chamber in a single GEM configuration. A sketch of the final detector configuration can be seen in figure 6. A mixed alpha source containing 239 Pu, 241 Am and 244 Cm is used for the test which was placed on top of a mesh cathode. The source measures 25 mm in diameter, 0.5 mm in height and the diameter of its active area is 7 mm. The active area is made smaller by partly shielding its surface with copper tape to reduce the alpha rate. The reason for this is that with lower source rate settings with higher discharge probabilities can be using the measurement methods discussed in section 2.2. The source fixed on top of the mesh using Kapton tape. A picture of the source and its spectrum can be seen in figure XX. The source emits alpha particles with the weighted energies of 5.155 MeV for 239 Pu, 5.486 MeV for 241 Am and 5.805 MeV for 244 Cm [3]. The alpha rate measured by the detector is 29.9 Hz.

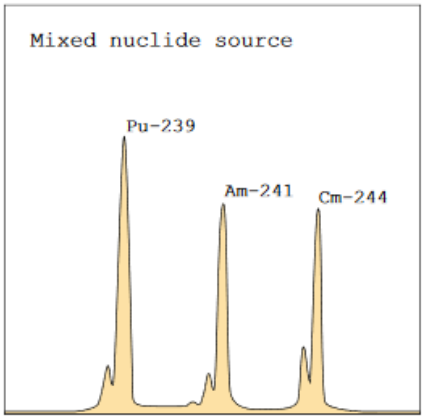

Figure 5: The emission spectrum of the mixed alpha source [3]

The distance of the drift gap is kept at a constant 35.5 mm with a constant drift field of 400 V/cm being applied in this gap throughout the measurements. On top of the THGEM a cover electrode was also implemented to mitigate the charge up effects of the inactive PCB material [22]. Below the foil there is the anode electrode. A single-pad anode, used as an readout electrode in a normal detector operation, is placed 2 mm below the THGEM. it should be noted, however, that in the course of the following studies all signals are read-out on the bottom side of the THGEM which allows to measure an absolute gain of the detector. Thus, the field between the bottom side of the THGEM and the anode was set to zero.

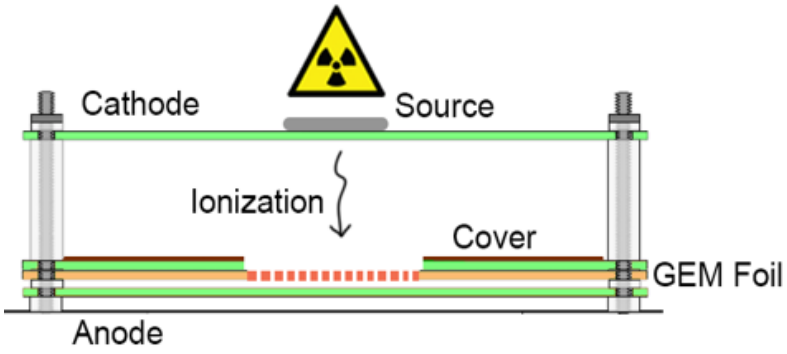

Figure 6: Schematic of the THGEM Detector

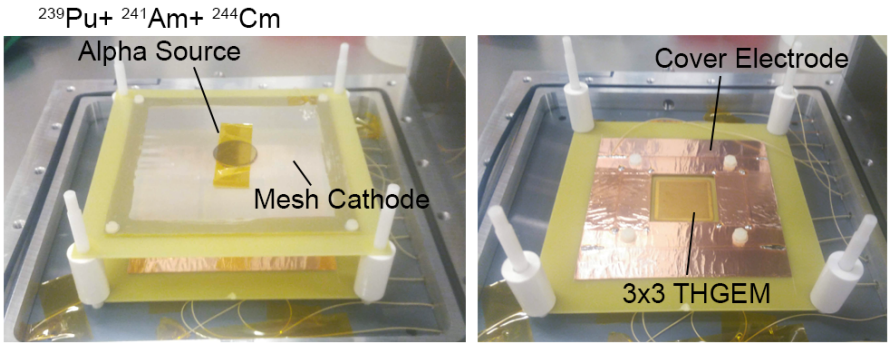

Figure 7: Pictures of the THGEM Detector

2.2 The measurement methods

To get a comprehensive understanding of the performance of the THGEM foil, two of its properties were measured when operating with four different gas mixtures. These gas mixtures include; Ar-CO_2 with gas ratios of 90-10% and 70-30%, Ne-CO_2 90-10% and finally Ar-CH_4 50-50%. The first three gas compositions are chosen in the characterization of the THGEM since these are the most common mixtures being used in experiments with GEMs. The latter (Ar-CH4) is used in the COMPASS RICH detector based on THGEM technology [23].

The first property to be measured when characterizing the THGEM is the gain of the foil as function of the applied voltage across it. Gain is effectively equivalent to the amount of signal amplification achieved by the detector and can be measured using the following formula:

$$Gain = \frac{I_{amp}}{I_{prim} - I_{off}} \tag{1}$$

The primary current (I_{prim}) corresponds to the raw signal from the ionization electrons on the top side of the foil before any avalanche multiplications occur. The amplification current is measured on the bottom side of the THGEM and is induced by many electrons which are created in the GEM hole by the avalanche multiplication effect. The total gain of the THGEM is given by the ratio of the amplification (I_{amp}) and primary currents. The radiation source generates primary current of approximately 0.7 pA. This very low current is measured using a Kiethley 6517B electro-meter [24] in a low-noise environment. The value of primary current is corrected for the offset (I_{off}) measured before applying potential to the electrodes.

Secondly the discharge probability (P_{Dis}) is measured. This measure dictates the likeliness of discharges occurring during operation per every event. Discharge probability is usually discussed as a function of gain as it is usually important to operate the detector with as much gain as possible while avoiding any possibly damaging discharges.

$$P_{Dis} = \frac{R_{Dis}}{R_{\alpha}} \tag{2}$$

As shown in the formula (2); by counting the rate of discharges (R_{Dis}) that occur during operation for the given gain setting and knowing the emission rate of the radioactive source (R_{α}), one can approximately calculate the probability of a discharge happening per alpha particle impinging the detector. The discharge rate is measured by counting the elapsed time where a given amount of discharges occur. The electrical signal read via the anode to capture the individual discharge events. The signal is passed first through a discriminator then a gate generator to achieve a uniform signal for each discharge, which are then counted with a threshold counter.

The current and rate values are repeatedly measured whilst varying the potentials across the foil where all the other parameters, such as drift and induction fields, are kept constant. The gain and discharge probability values are then calculated with the given formulas. By doing so a characterization of the THGEM for each gas was achieved. The statistical errors for these values are then also calculated assuming discharge occurrence undergoes Poisson distribution.

2.3 Results

The resulting gain curve plot from the THGEM measurements for all the measured gas mixtures is shown in figure 8

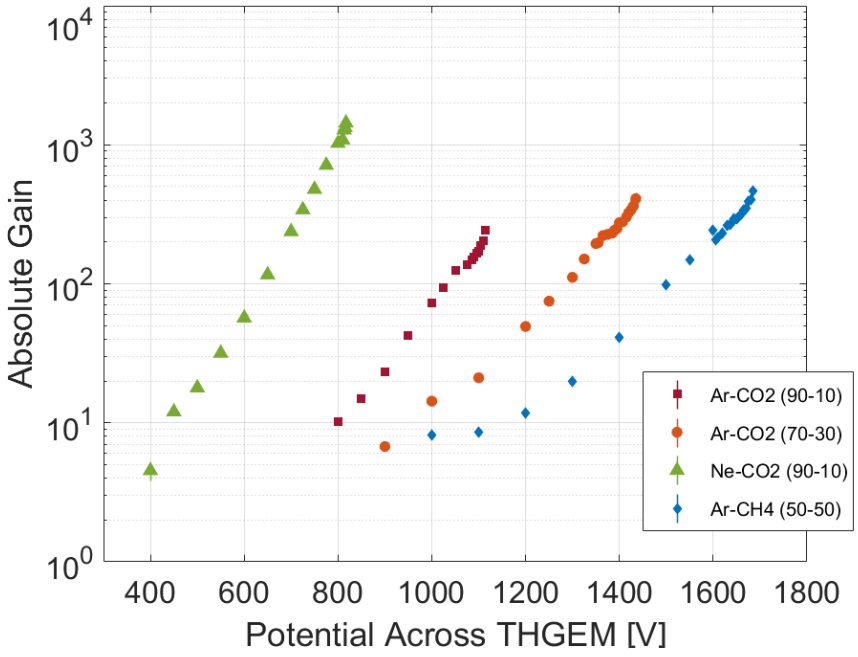

Figure 8: Gain measurements for THGEM with four different gas mixtures

The gain behaviour matches the expectation the results from measurements conducted on normal GEM foils. The gain shows an exponential increase with applied voltage across the foil. The gas mixture with a greater portion of quencher leads to a lower gain for the same applied voltage as is evident by comparing curves of the two Ar-CO_2 mixtures. Gain of the Neon based mixture is higher due to the larger value of Townsend coefficient for this noble gas.

An observation that couldn't be fully explained yet is the breaking of the exponential trend in the high gain regions. The gain value seems to drop at a certain point and rises again back to the trend level afterwards. This dip in the gain curve corresponds exactly to the point where discharges start occurring. Thus, it is hypothesized that this dip is caused by or at least is correlated to the discharge events. However, to determine if the discharges

really cause a shift in the gain level of the detector or if the measurement process gets effected by the discharge events a study of the discharge signals is conducted.

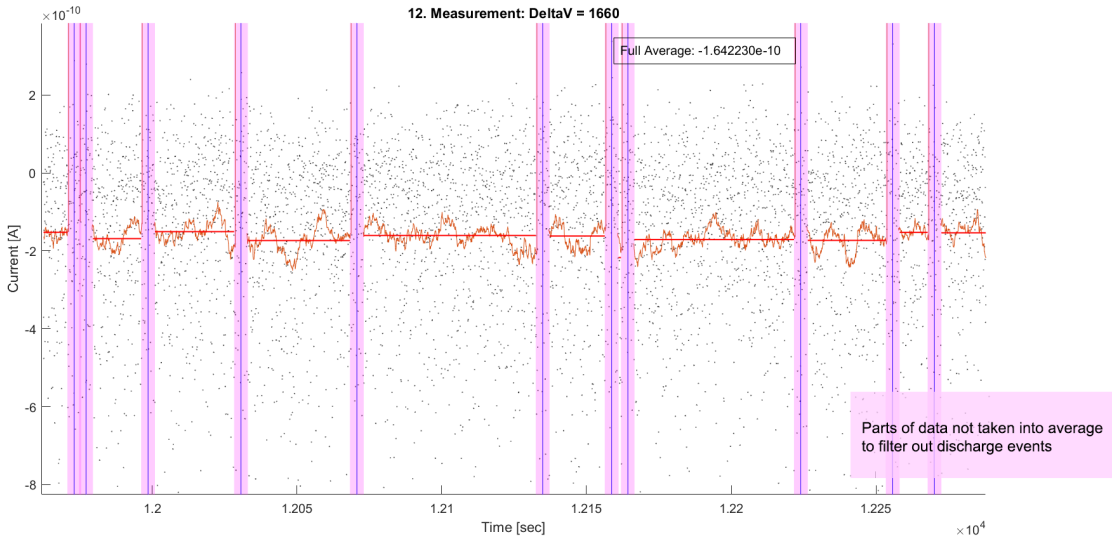

Figure 9: An example current measurement with discharges

The aim of this analysis is to separate the data points that are possibly effected by the spike from the discharges. The amplification current (I_{amp}) needed for the measurement of the gain is calculated by averaging the current at the bottom side of the THGEM. Discharge events affect this current in form of large spike signals. In figure 9 an example measured current for a given voltage setting is shown. The average current value from this measurement (after the calculations in formula 1) corresponds to one point in the gain plot in figure 8. The spikes in the signal caused by the discharge events are shown as the vertical lines coloured dark blue. Eleven discharge events can be observed for this measurement. On either side of the discharges the region of the filtered out data points is indicated with pink. 60 data points before and after the occurrence of discharges are filtered out. The orange graph shows the moving average over 50 data points. The red lines indicate the average level of the section between two discharges.

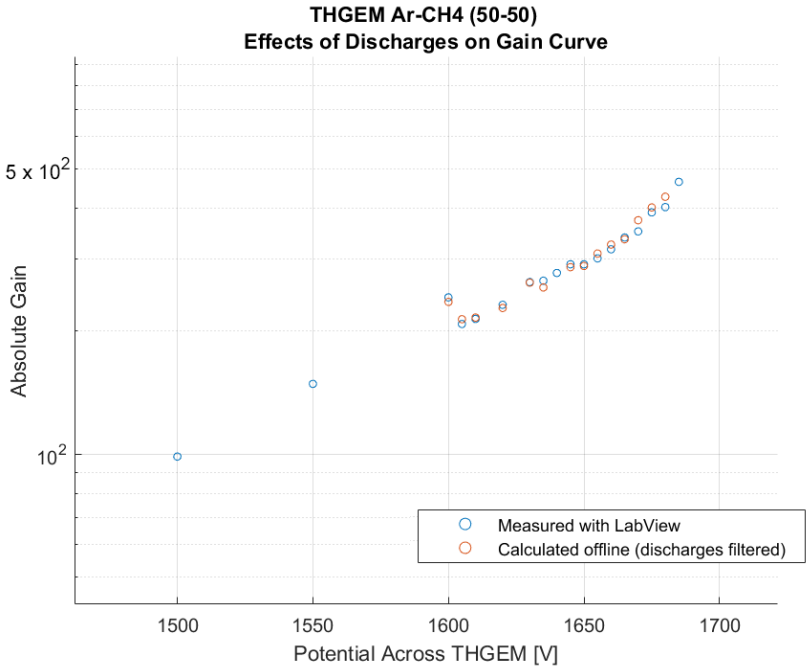

Figure 10: Gain measurement for Ar-CH_4 with and without discharge filtration

In figure 10 the result of the discharge filtration is given. The Ar-CH_4 measurements are chosen as an example but similar results were also observed with Ar-CO_2 (90-10) gas mixture as well. As can be observed in this plot, for both cases the obtained averages deviate very little from one another and show the previously effect of the breaking of the exponential behaviour. With the fact that this effect is still observed even after the data points around discharges aren't taken into account, it is shown that this phenomenon is not a measurement error. The underlying mechanism for this sudden drop in the gain is still not understod and is under investigation.

The results from the discharge probability measurements on the THGEM introduced earlier is shown in figure 11.

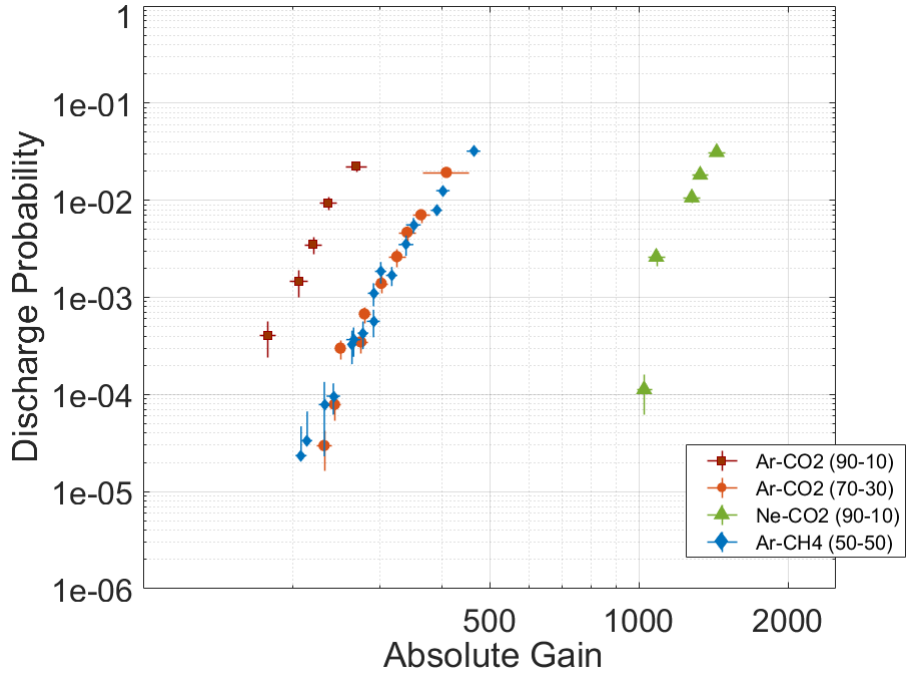

Figure 11: Discharge probability measurements for THGEM with four different gas mixtures

For the THGEM measurements the expected discharge probability shape for all the gases can be seen. Comparing the two Ar-CO_2 mixtures for example, it can be seen that the gas mixture with a greater portion of quencher leads to a lower discharge probability for the same gain. One interesting thing to note is however that Ar-CH_4 and Ar-CO_2 (70-30)% have very similar discharge probability behaviours. Normally methane is known as a better quencher than CO_2. These measurements indicate however that for this setup methane is worse at mitigating discharges, since performs the similarly even though it has a greater portion in the mixture.

To be able to make more sense of this provided data a comparison of THGEMs with normal GEMs regarding discharge probability is given. Figure 12 shows a comparison of the THGEM results with the discharge probability curves obtained with standard GEMs in [4]. The measurements for the standard GEM incorporate a GEM with 50 μm thick polyimide foil with 50 μm inner hole diameter and a pitch of 140 μm.

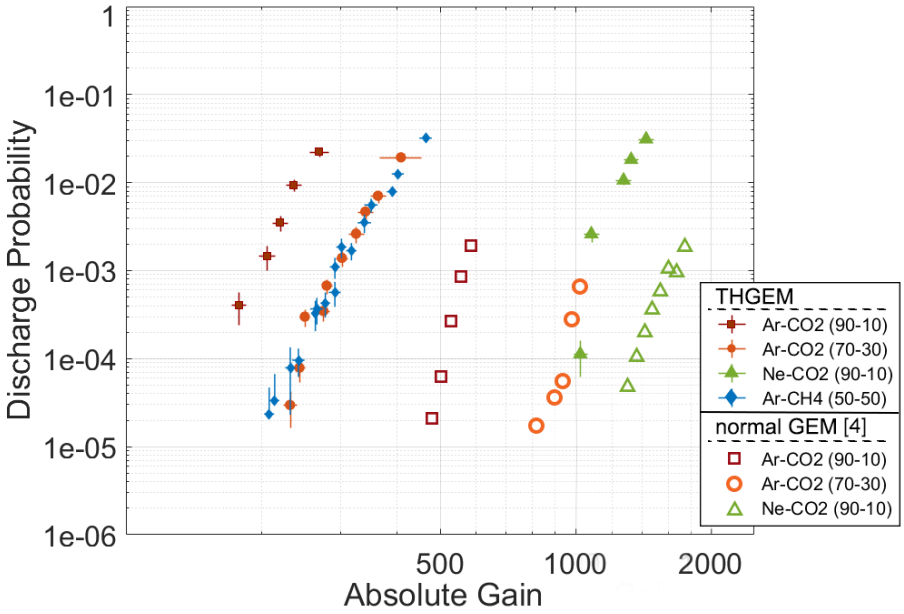

Figure 12: THGEM discharge probability compared to the values obtained with standard GEMs (from [4]).

For three mixtures, where the comparison is possible, the THGEM shows systematically higher discharge probability than standard GEM at the same gas gain. It is worth to mention at this point that this result fits the current intuitive understanding of discharge formation. Discharges are thought to occur when the amount of charges in the GEM hole exceeds a certain critical level. Since THGEMs have smaller number of holes per given area because of their bigger hole diameter. This would mean that a greater number of charges is expected to go into a single THGEM hole in comparison to a normal GEM hole under the same gain settings. Further investigation of this in form of simulation and testing with more samples is ongoing.

3 Optical Read-Out System

GEM detectors are very fragile against electrical discharges. They can very easily be damaged during operation, sometimes even irreparably, if the necessary precautions are not taken. This weakness combined with the fact that for many applications they are required to be operated for long durations and in very high gain settings makes the task of discharge mitigation especially important.

Because of this throughout the years many strategies have been developed to protect the GEM foils against discharges. These include; using protective resistances to reduce the high currents that would normally be achieved during discharge events, or to use multiple foils in a stack configuration to be able to achieve high gains even when operating each foil in relatively low gain. These methods have both proven to be very useful at increasing the robustness of GEMs against discharges and using these modifications GEMs are being implemented in modern high rate particle and nuclear physics experiments to be operated at extreme conditions. Thus, it can easily be said that the practical expertise for increasing GEM stability is readily available.

However, the physics of the formation and especially propagation of discharges in GEMs is not yet fully understood. To optimize our current detector designs it is crucial to gather a similar level of theoretical understanding of discharges. There have been many huge leaps in this direction by means of analysing the electrical signals created during discharges or by simulating discharge events. The findings using these methods have been previously introduced in chapter 1.2.

In search of new methods for inspecting discharges, it has been proposed to use the now readily available CMOS or CCD based optical read-out systems as an alternative to the classic electronic read-out. The main advantage of optical read-out systems is the very high spatial resolutions achieved by the high granularity of the used imaging sensors. The images acquired with this method are also more intuitive to analyse compared to the signals acquired by electronical read-out. Furthermore, optical read-out coupled with GEM detectors or other MPGDs have already been shown to be very effective in many areas including particle tracking in nuclear physics and radiography in medical physics [25, 5]. For these reasons implementing various optical read-out systems to study discharges is regarded as an exciting new method in the field.

As an example, a group from the University of Zagreb recently recorded the evolution of secondary discharges in a single hole THGEM using a very high-speed CMOS scientific camera [26]. The observations made by using this method offered a completely new perspective on the discharge propagation event and rekindled the important discussions regarding the mechanisms behind it in the scientific community. In a similar fashion a project of developing an optical read-out system using a scientific CMOS camera to capture discharge propagation events was initiated in TUM. In the following chapter the design and production of the detector needed for this project and the initial tests of operating it by capturing images of alpha tracks will be discussed.

3.1 Design and production of the optical read-out system

A GEM detector with optical read-out works by capturing the scintillation light emitted from excited atoms during the avalanche multiplication process with an imaging sensor. This simple concept lets us get a glimpse of the trajectories of even the tiniest of particles like electrons. A hard task which previously required large setups like bubble chambers to get good results. With advancements in the imaging sensor technology in the silicon era, a much smaller detector can capture similar track images in digital format.

In the designing of such a detector with optical read-out there are mainly four challenges to be overcome. These include:

i) achieving enough charge multiplication from the initial ionisation events to produce a detectable amount of scintillation photons,

ii) making sure the wavelength of these scintillation photons lie within the detectable spectrum of the used imaging sensor,

iii) making the detector light tight as much as possible to reduce the background noise,

iv) choosing the proper camera equipment to capture the very dim light from the multiplication events.

The design and production process to overcome these challenges is discussed in this section.

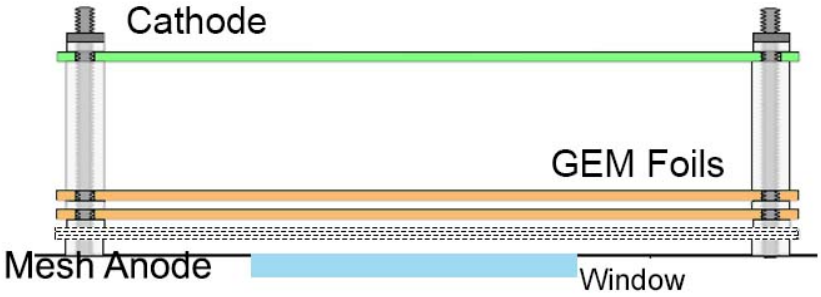

Figure 13: Schematic of the used GEM detector configuration

The optical read-out system was implemented as an addition to a GEM detector as previously introduced. Here the amplification from the GEM foils is the source of the scintillation light required for the imaging. For this project the detector setup (earlier being used for the characterisation of a THGEM [see chapter 2]) was modified. To have higher spatial resolution normal GEM foils with an active are of 10x10 cm^2 were used instead of the 3x3 cm^2 THGEM. Furthermore, a two GEM setup was implemented to achieve high enough gains for good signal o background ratio. The top foil (GEM1) has a large pitch (280 μm) and the bottom foil (GEM2) has a small pitch (90 μm)geometry. The mesh electrode, previously being used for the THGEM measurements as a cathode was installed this time as the anode. The reason for this being, a see-through mesh anode allowing the bottom side of GEM2 to be viewed from below. Also, a window hole was drilled in the bottom plate of the detector box for the same purpose. The window is circular in shape and is made of an uncoated BOROFLOAT glass disc [27], which was glued airtightly to the detector. This way, the gas system for the GEM is separated from

the camera housing.

The main process of the signal amplification in GEMs come in form of avalanche multiplication of the initial ionisation electrons as they enter the GEM holes. Inside the GEM holes electrons accelerate to very high energies from the strong ambient electrical field. The electrons then ionize more gas atoms resulting in charge multiplication. However, this is not the only possible process for the electrons to lose their energy. The electrons can also excite the gas atoms without causing an ionisation. These excited atoms can then in turn de-excite by emitting scintillation photons. The wavelength of the scintillation photons depends on the available electron orbitals of the gas atom. Usually with GEMs using Ar-CO_2 mixtures (or the other previously introduced gas mixtures) the emitted scintillation photons have a wavelength in the ultra-violet region of the light spectrum. For this reason, the light from the avalanche events can't be seen or be detected with the available CMOS camera when operating with the classic gas compositions. However, by changing the used gas mixture it is possible to shift the wavelength in to visible light to match the quantum efficiency of the imaging sensor. Usually gas mixtures with CF_4 as the quencher are used to achieve this result. In figure 14 the light emission spectrum of the used Ar-CF_4 (80-20) mixture can be seen. As needed for the project, the secondary scintillation peak lies in the visible light region, which also matches the quantum efficiency of the sCMOS (scinetific Complementary Metal-Oxide-Semiconductor) sensor of the used scientific camera. With this, using CF_4 grants the possibility of using the scintillation photons for particle detection and track imaging is available.

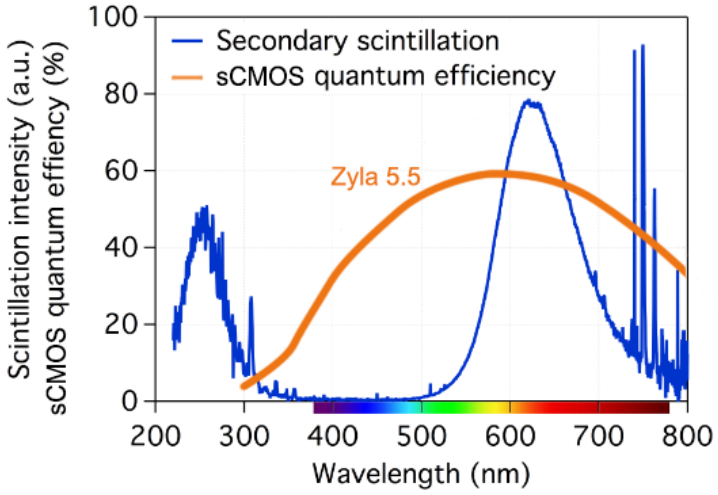

Figure 14: Secondary scintillation spectrum of Ar-CF_4 (80-20) [5]

Regarding the assembly of the optical read-out system one the biggest parts needed to be produced is the light tight housing for the camera. Achieving a good level of light tightness is crucial to obtain proper signal-to-noise ratios in the acquired images.

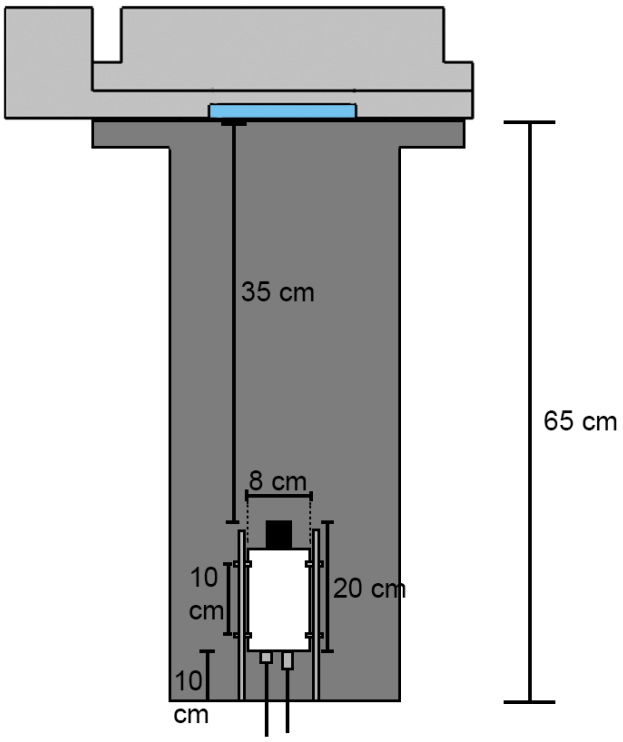

Figure 15: The technical drawing of the camera housing

For this reason the camera is housed inside a long aluminium cylinder, which is attached to the detector box facing the window on one side and has a cable outlet hole for the camera on the other side. The cylinder has a length of 65 cm. The reason for the larger design is to have enough space to adjust the distance between the camera and the GEM foil if needed. The camera is fastened inside the cylinder to mounting bars on both its sides with butterfly screws. The camera is positioned 35 cm away from the detector to match the focusing capabilities of the used camera lens. Both ends of the cylinder are screwed shut when in operation, with the possibility of adding O-Rings inside the contact areas to improve the light tightness even further. Being the only opening in the housing, the hole for the camera cables on the bottom is then sealed with black masking tape. With all these measures taken, an almost complete pitch-black interior for the detector was achieved. The remaining little background noise visible in captured images are caused by the internal electrical noise of the imaging sensor itself and isn't caused by any light leak-in from the outside.

Figure 16: The detector with the camera housing

Regarding the camera equipment, a Zyla 5.5 scientific camera from ANDOR was chosen. It has a 5 Megapixel – 22 mm diagonal sCMOS (scientific CMOS) sensor and is operated via a USB 3.0 link to the computer. The sCMOS technology used in the camera has extremely low noise and wide dynamic range (comparable to CCD based equipment) in low-light imaging. CCD technology is usually preferred over normal CMOS for similar scientific applications as this project. One of the main reasons for this is the rolling shutter problem with the usual CMOS architecture. Rolling shutter refers to the fact that with CMOS cameras pixels on the sensor grid are read row-by-row, so different rows of pixels capture information from different time instances. For applications with fast moving objects or rapidly changing scenes this property can result in unwanted temporal aliasing effects in the image. Nevertheless, the Zyla 5.5 also has a global (snapshot) shutter mode, where all the pixels are read out simultaneously, mitigating such unwanted effects. Moreover, the camera has multiple triggering modes, each suited for different applications. These include; internal shutter, software shutter, external shutter and external exposure. For example, whilst in software shutter mode, triggering of image acquisition and the configuring of the camera settings are done manually with the software. For the application of capturing tracks however such a manual triggering mode wouldn't be useful since the events to be captured occur very randomly and disappear quickly. External

exposure mode on the other hand is much more suited for this task. With this mode the triggering instance and the exposure duration is given to the camera by an external logic signal. For the setup in discussion this signal comes from the electronical read-out in the GEM detector, which goes through a gate generator to be properly shaped. All the listed features of the camera combined with the fact that CMOS based cameras are usually much more economic than their CCD counterparts made the Zyla 5.5 a very fitting equipment for this project.

Figure 17: Andor Zyla 5.5 camera

As a final note on the operation process of the optical read-out; the camera is controlled using the μManager software [28, 29]. All the previously introduced settings and operation modes of the camera can be selected using the software without a need to access the camera in person. This enables very rapid testing to find the optimal configuration of the said settings. The software also has multiple ways of storing and displaying the captured images. For example, by using the 16-Bit file format to save the acquired images it is possible to make use of the full potential of the camera in terms of dynamic range with the cost larger file sizes of the images. Moreover, μManager also has some additional features beyond being able to operate the camera. As an example, it is possible to select which part of the frame will be captured when acquiring images by defining a region of interest. By limiting the field of view using this method it is possible to increase the frame

rate of the camera. Other than that, as a way of quickly analysing the captured images, the software also has the capability to plot the pixel value profile over a line segment set by the user on a given image. This feature was seen to be especially useful when capturing alpha tracks (see chapter 3.2). Additionally, the software comes with the ImageJ plugin. A tool, that is very useful for quickly editing the captured images in terms of brightness and contrast adjustments without needing additional graphics editor software.

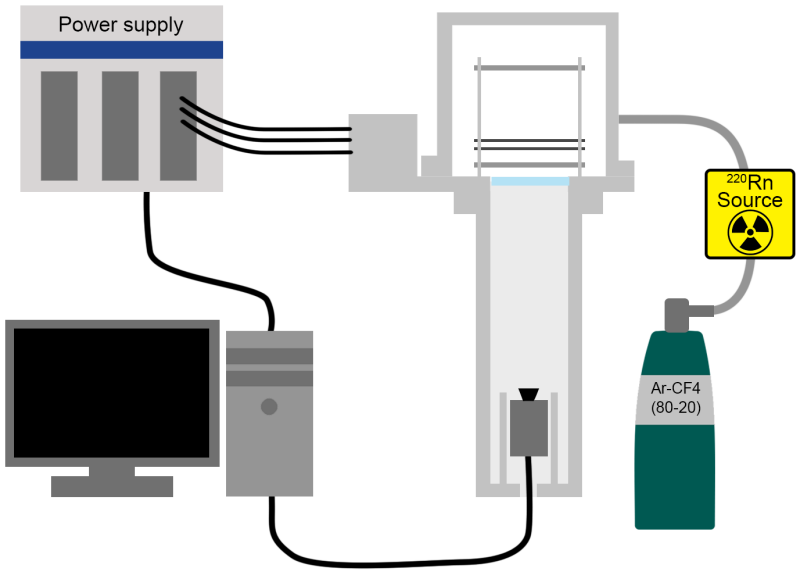

Figure 18: Diagram of the optical readout setup

3.2 Alpha particle tracking

After the production process of the read-out system was completed, it was devised to test the detector by capturing alpha particle tracks. This would lead to gathering experience on operating the optical read-out system and testing its capabilities as a preparation for the planned discharge studies.

Commissioning of the setup was done using an alpha emitter, ^{220}Rn. Alphas are helium-4 nuclei and are a type of highly ionizing particles [30]. They are emitted as nuclei undergo alpha decay. Because of their relatively high mass, alphas can't propagate long distances as they pass through matter and lose their energy rapidly through ionisation of the surrounding medium. According to Bethe-Bloch formula, the energy loss of particle increases with its decreasing velocity. This fact leads to the well-known Bragg peak shaped energy loss behaviour of the particle, where the particle loses maximum energy just before it stops. As a result of this, alpha tracks have a very distinct, easily recognisable shape, making them very suited for testing the optical read-out system. The radon alpha source (^{220}Rn), which is in gas form in room temperature, was mixed into the gas input of the GEM detector. This way, a low rate of alphas can be attained within the detector chamber. The alphas are emitted randomly in the detector chamber, leading to tracks in many orientations and sizes.

A selection of the captured alpha track images are given below. These images are not shown in the raw form as they are captured by the camera but are edited. Their brightness and contrast values are set in a way to make the tracks more visible and the background noise around the tracks is also darkened. Nonetheless the shapes of the tracks and brightness profile along them are untouched. Also, the tracks are usually much smaller in comparison to GEM foil, which spanned the field of view of the camera, so the images were cropped to fit the track size.

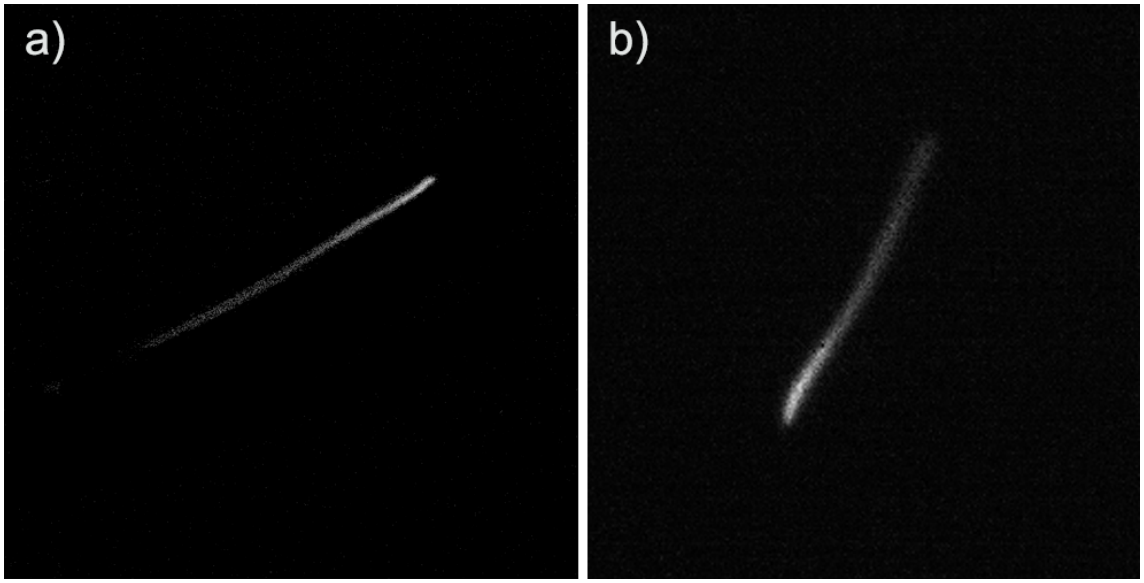

Figure 19: Images of alpha tracks captured with the optical read-out

Image a) in figure 19 shows what can easily be labelled as "The classic alpha track". Among all the dozens of recorded alpha tracks this kind of track shape was by far the most common. With the absence of an outer strong magnetic field, the alphas are observed to propagate through the gas linearly as expected. The track starts very dim and gets brighter towards its end where it gets the brightest. This will be discussed in more detail below. Image b) also shows a similarly shaped alpha track.

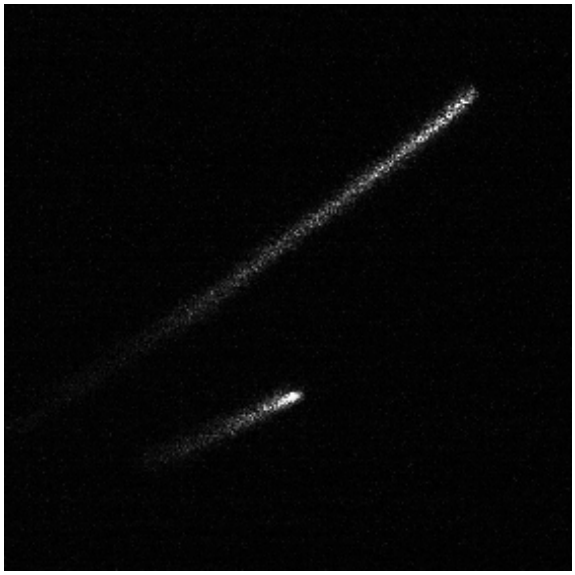

Figure 20: Two alpha traks captured in the same exposure

In figure 20 two tracks can be seen. These alpha particles are thought to be uncorrelated in their emission and are captured during the same exposure. In comparing of the two tracks, it can be observed that they don't share the same size, even though the individual alphas should have very similar initial kinetic energies. Such size differences appear because of the different inclination angles of the two tracks. The alphas are emitted randomly in the detector chamber and thus can propagate in different directions.

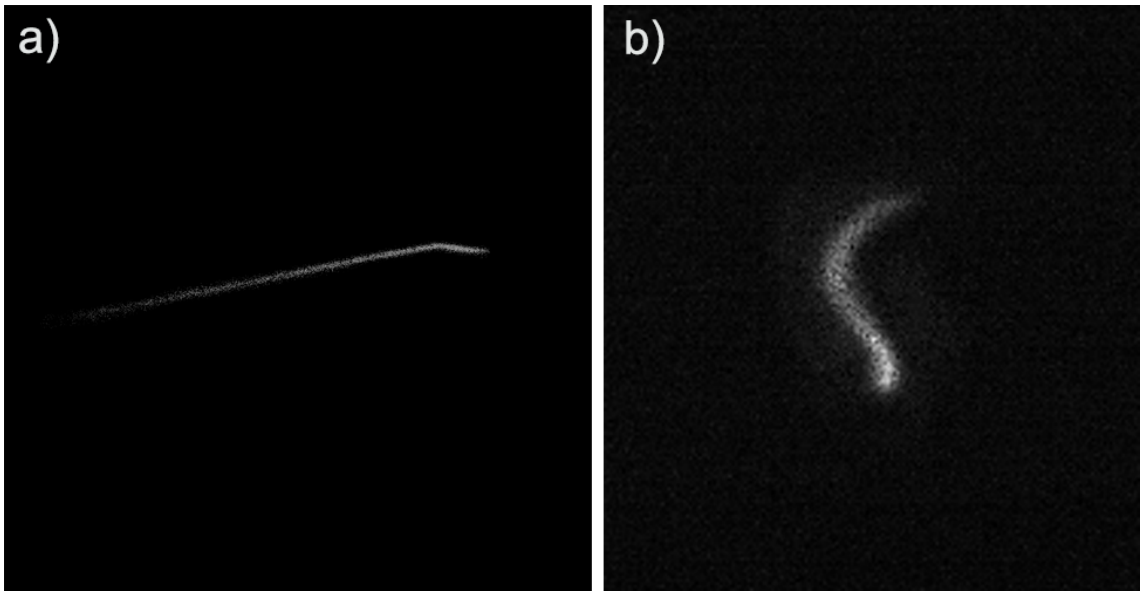

Figure 21: Alpha tracks with scattering event

Image a) in figure 21 shows an alpha track with an observable kink. These kinks in-

dicate collision events with large momentum transfer between the alpha particle and the gas medium. These kinks are usually observed to be located towards the end of the track where the kinetic energy of the alpha particle is lower. At these lower energies, the deflection angle after the collision can be larger, making the kink much more evident. Finally, on the last picture a very bizarre and much rarely observed track shape is shown. The swirliness of its trajectory is thought to be caused by the combination of all the previously mentioned effects, including; the track being shaped by the drift field and appearing shorter because of a more vertical inclination as well as the particle undergoing maybe even multiple collisions with large momentum transfers.

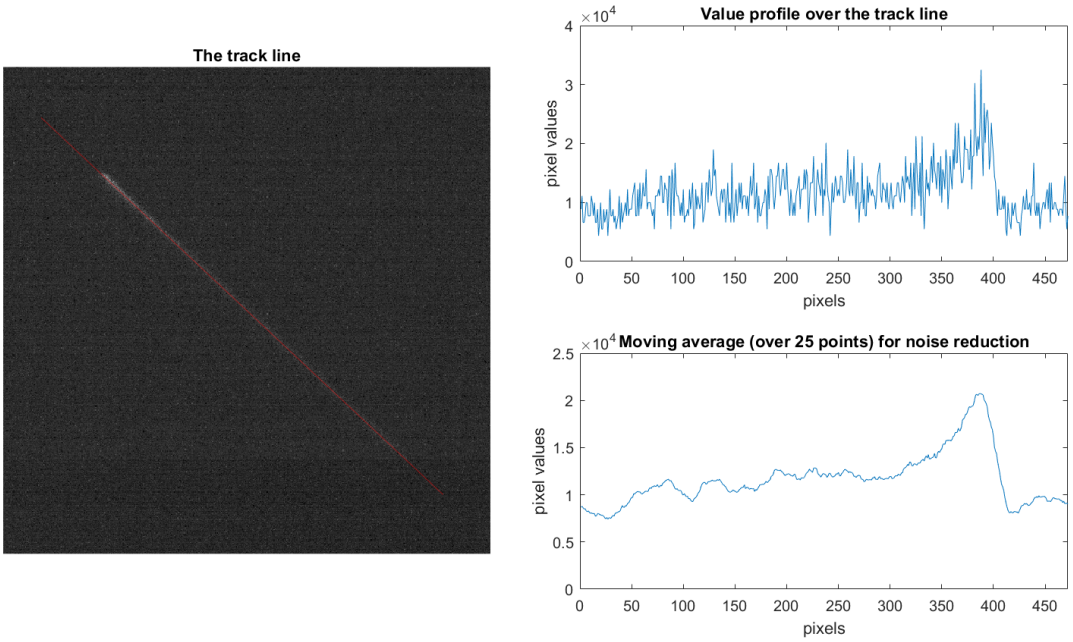

Figure 22: Bragg peak like profile over the track line

In Figure 22 a classic alpha track with the value profile along it is shown. The track photo is unprocessed and contains the original background noise. On the top plot a profile of the pixel values along a line segment (shown in red) on top of the track is given. The pixel number zero corresponds to the bottom right end of the line, and pixels are counted towards the other end in a linear fashion. The bottom plot displays the moving average over 25 points on the profile. This is done to subdue the fluctuations on the top plot and thus to get a more smoothed out, less noisy profile of the pixel values. In both plots the Bragg shape of the profile is very clear. The brightness along the trajectory gets gradually larger, later at the end of the track the brightness peaks and disappears abruptly. This observation fits very nicely to the expectation and the theory, where the energy deposited by the alpha increases as it progresses through the medium. This energy deposition takes place in form ionisation and this mechanism stops once the kinetic energy of the alpha drops below of the needed ionisation energy of the gas. The GEM holes, which have

more ionisation events occurring overhead of them are seen brighter, since the amount of avalanche multiplications depends on the entering charge count.

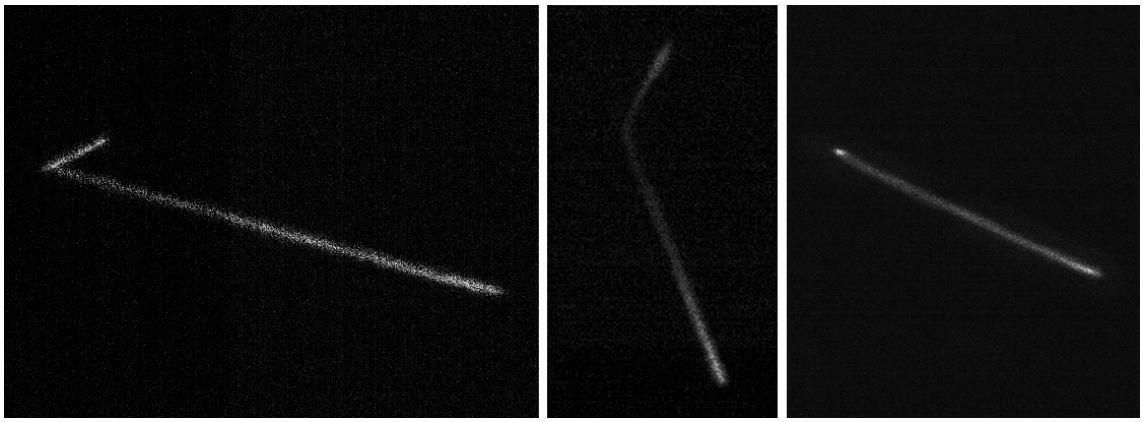

Figure 23: The emissions of a second alpha particle during the decay of ^{216}Po to ^{212}Pb

The final observation made regarding alpha tracks is shown in Figure 23. On some instances two alphas that are emitted from the same point were spotted. The pictures display some examples of this with different track orientations (the rightmost image showcasing one branch completely perpendicular to the imaging plane seen as bright point). Such track formations are not too commonly captured with the very short exposure times used at acquiring all the shown images, however gets more frequent as the exposure time is increased. This observation can be explained with the decay chain of the used radiation source (shown in Figure 24). The primary alpha source for this experiment; ^{220}Rd decays to ^{216}Po emitting an alpha in the process [6]. These alpha particles correspond to the main branch shown in the images. Additionally, the newly created 216Po, having a short half-life of 140 milliseconds, can also undergo an alpha decay to ^{212}Pb. Because of the short time scales needed for the second decay event to occur, a second alpha particle can be emitted effectively right after the first one. This second track can then be captured within the same exposure by adjusting the exposure duration accordingly.

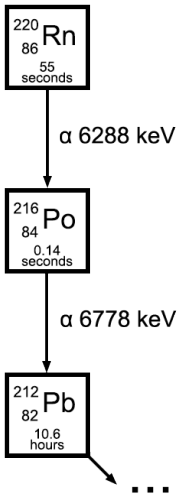

Figure 24: Decay chain of ^{220}Rn [6]

With these observations the initial test of capturing alpha track photos using the optical read-out system was concluded. The initial goal of gaining experience and creating know-how on operating the detector within the group was accomplished. The detector can perform as initially devised and is ready to be used for the planned discharge studies.

4 Summary and Outlook

In the course of this thesis two main tasks were undertaken. The characterisation of a 3x3 cm^2 THGEM foil and the development of an optical read-out system for a GEM based detector.

For the characterisation of the THGEM foil four gas mixtures were used. These being Ar-CO_2 (90-10 & 70-30), Ar-CH_4 (50-50) and Ne-CO_2 (70-30). The two measurements of gain and discharge probability were conducted iteratively over a large applied voltage region and with multiple repetitions. The unexpected observations such as the breaking of the exponential trend of gain after the occurrence of the first discharges during the measurement were examined in detail to make sure of the reliability of the measurements. The results from the stability studies indicate that THGEMs perform worse in terms of discharge probability in comparison to standard GEM foils. THGEMs have shown to have 2-3 orders of magnitude higher discharge probability for the same gain level as standard GEMs. This very crucial under performance of THGEMs is explained by the lesser count of holes on the foils, where a greater amount of charges accumulates in each hole, increasing the probability of exceeding the charge threshold before discharges. This result is of importance for the MPGD community for optimizing future detector architectures and is being further investigated beyond the scope of this thesis in form of simulations. Also, the measurements conducted for the 3x3 cm^2 THGEM are planned to be replicated with different THGEM foils before finalizing the comprehensive stability characterisation of the THGEMs.

During this thesis an optical read-out system was also implemented. It incorporates a CMOS scientific camera that captures the scintillation light emitted during the avalanche multiplication process inside the GEM holes. The gas mixture containing CF_4 as quencher is used to match the wavelength of the emitted light to the quantum efficiency of the used imaging sensor. After its assembly the optical read-out system was tested by being used to capture tracks of alpha particles. During this period the know-how needed to perform the wanted measurements with the equipment was gained. Many interesting results were also gained from the examinations of alpha tracks. The energy deposition of the alpha particle was shown to be in accordance to the Bragg curve. Furthermore, a secondary alpha decay after the first decay event of ^{220}Rd source was also observed. This was explained by the capturing of the decay of ^{216}Po, an isotope with relatively short half-life, within the same exposure. The optical read-out system performed according to the initial expectations during the imaging of alpha tracks. It was seen to capture detailed images in very low light conditions achieved with the light tight design of the produced camera chamber. Plans for the future with this new very versatile system include using it for imaging discharge propagations. The optical read-out will be a new probing method for and will shed new light on this not fully understood phenomenon.

5 Acknowledgements

First and for most I would like to thank my supervisor Dr. Piotr Gasik for his constant support throughout this thesis. I couldn't thank him enough for the patience and great feed-back he has given and of course for sharing his immense expertise on the field of experimental physics at all times. I would also like to thank Prof. Fabbietti for giving me the opportunity to become a part of this very friendly and joyous group. I also want to thank Prof. Kienberger for reviewing this thesis and for his constant friendliness throughout the process. I want to thank Emma Chizzali for helping me throughout the design and measurement process and for being a constant support. I want to thank Ralf Lang for his vast help with the design and production of the camera housing. The optical read-out project wouldn't be possible without him. I would also like to thank Lukas Lautner, Thomas Klemenz, Andi Mathis and Berni Hohlweger for giving such joy and for being so helpful over the whole period of this thesis. I want to thank all the members of the Dense and strange matter family for all their support. Finally, I want to thank all my friends and especially family for cheering me at all times.

References

[1] Fabio Sauli. The gas electron multiplier (gem): Operating principles and applications. *Nuclear Instruments and Methods in Physics Research Section A: Accelerators, Spectrometers, Detectors and Associated Equipment*, 805:2–24, 2016.

[2] P Gasik. private communication.

[3] E Ziegler. Alpha spectrometry sources. URL `http://www.ezag.com/fileadmin/ezag/user-uploads/isotopes/isotopes/Isotrak/isotrak-pdf/Product_literature/EZN/04_section04_alpha_spectrometry_sources.pdf`.

[4] P Gasik, A Mathis, L Fabbietti, and J Margutti. Charge density as a driving factor of discharge formation in gem-based detectors. *Nuclear Instruments and Methods in Physics Research Section A: Accelerators, Spectrometers, Detectors and Associated Equipment*, 870:116–122, 2017.

[5] FM Brunbauer, M Lupberger, E Oliveri, F Resnati, L Ropelewski, C Streli, P Thuiner, and M van Stenis. Radiation imaging with optically read out gem-based detectors. *Journal of Instrumentation*, 13(02):T02006, 2018.

[6] J Porstendörfer. Properties and behaviour of radon and thoron and their decay products in the air. *Journal of Aerosol Science*, 25(2):219–263, 1994.

[7] Fabio Sauli. Gem: A new concept for electron amplification in gas detectors. *Nuclear Instruments and Methods in Physics Research Section A: Accelerators, Spectrometers, Detectors and Associated Equipment*, 386(2-3):531–534, 1997.

[8] M Inuzuka, H Hamagaki, Kyoichiro Ozawa, T Tamagawa, and T Isobe. Gas electron multiplier produced with the plasma etching method. *Nuclear Instruments and Methods in Physics Research Section A: Accelerators, Spectrometers, Detectors and Associated Equipment*, 525(3):529–534, 2004.

[9] Fabio Sauli. Principles of operation of multiwire proportional and drift chambers. In *Experimental Techniques in High-energy Nuclear and Particle Physics*, pages 79–188. World Scientific, 1991.

[10] F Massines, N Gherardi, N Naude, and P Segur. Glow and townsend dielectric barrier discharge in various atmosphere. *Plasma physics and controlled fusion*, 47(12B):B577, 2005.

[11] András László, Gergő Hamar, Gábor Kiss, and Dezső Varga. Single electron multiplication distribution in gem avalanches. *Journal of Instrumentation*, 11(10):P10017, 2016.

[12] P Gasik. Development of gem-based read-out chambers for the upgrade of the alice tpc. *Journal of Instrumentation*, 9(04):C04035, 2014.

[13] David J Nowak, James E Rice, and Donald R Bianco. Ion gating grid, April 17 1979. US Patent 4,150,319.

[14] D Mörmann, A Breskin, R Chechik, and D Bloch. Evaluation and reduction of ion back-flow in multi-gem detectors. *Nuclear Instruments and Methods in Physics Research Section A: Accelerators, Spectrometers, Detectors and Associated Equipment*, 516(2-3):315–326, 2004.

[15] Jeremie Merlin. Effect of discharges on gem detectors- single hole setup, 2018. Presentation in RD51 Collaboration Meeting 2018 Munich. URL `https://indico.cern.ch/event/709670/contributions/3008626/attachments/1672294/2683230/JMERLIN_RD51ColMeeting_GEM_DischargeEffects_24052018.pdf`.

[16] V Peskov, P Fonte, P Martinengo, E Nappi, R Oliveira, F Pietropaolo, and P Picchi. Advances in the development of micropattern gaseous detectors with resistive electrodes. *Nuclear Instruments and Methods in Physics Research Section A: Accelerators, Spectrometers, Detectors and Associated Equipment*, 661:S153–S155, 2012.

[17] S Bachmann, A Bressan, M Capeáns, M Deutel, S Kappler, B Ketzer, A Polouektov, L Ropelewski, F Sauli, E Schulte, et al. Discharge studies and prevention in the gas electron multiplier (gem). *Nuclear Instruments and Methods in Physics Research Section A: Accelerators, Spectrometers, Detectors and Associated Equipment*, 479(2-3):294–308, 2002.

[18] P Fonte, V Peskov, and B Ramsey. The fundamental limitations of high-rate gaseous detectors. In *Nuclear Science Symposium, 1998. Conference Record. 1998 IEEE*, volume 1, pages 91–95. IEEE, 1998.

[19] Heinz Raether. Electron avalanches and breakdown in gases. 1964.

[20] EE Kunhardt and Y Tzeng. Development of an electron avalanche and its transition into streamers. *Physical Review A*, 38(3):1410, 1988.

[21] V Peskov. Discharge phenomena in gaseous detectors, 2018. Presentation in RD51 Collaboration Meeting 2018 Munich. URL `https://indico.cern.ch/event/709670/contributions/3008581/attachments/1670690/2685706/Peskov_presentation_in_Munich.pdf`.

[22] Maxim Alexeev, R Birsa, F Bradamante, A Bressan, M Büchele, Michela Chiosso, P Ciliberti, S Dalla Torre, S Dasgupta, O Denisov, et al. The gain in thick gem multipliers and its time-evolution. *Journal of Instrumentation*, 10(03):P03026, 2015.

[23] Maxim Alexeev, R Birsa, F Bradamante, A Bressan, M Büchele, Michela Chiosso, P Ciliberti, S Dalla Torre, S Dasgupta, O Denisov, et al. Thgem-based photon detectors for the upgrade of compass rich-1. *Nuclear Instruments and Methods in Physics Research Section A: Accelerators, Spectrometers, Detectors and Associated Equipment*, 732:264–268, 2013.

[24] Tektronix. 6517b electrometer/high resistance meter. Datasheet for Keithley 6517B. URL `http://download.tek.com/datasheet/6517B-Datasheet_1KW-60280-1.pdf`.

[25] S Bachmann, S Kappler, B Ketzer, Th Müller, Leszek Ropelewski, Fabio Sauli, and E Schulte. High rate x-ray imaging using multi-gem detectors with a novel readout design. *Nuclear Instruments and Methods in Physics Research Section A: Accelerators, Spectrometers, Detectors and Associated Equipment*, 478(1-2):104–108, 2002.

[26] A Utrobičić. Usage of single hole thgem foil for delayed discharge propagation analysis, 2018. Presentation in RD51 Collaboration Meeting 2018 Munich. URL `https://indico.cern.ch/event/709670/contributions/3027853/attachments/1672132/2682893/Discharge_propagation_THGEM_v2.pdf`.

[27] Andrew A Wereszczak and Charles E Anderson Jr. Borofloat and starphire float glasses: A comparison. *International Journal of Applied Glass Science*, 5(4):334–344, 2014.

[28] Arthur Edelstein, Nenad Amodaj, Karl Hoover, Ron Vale, and Nico Stuurman. Computer control of microscopes using μmanager. *Current protocols in molecular biology*, 92(1):14–20, 2010.

[29] Arthur D Edelstein, Mark A Tsuchida, Nenad Amodaj, Henry Pinkard, Ronald D Vale, and Nico Stuurman. Advanced methods of microscope control using μmanager software. *Journal of biological methods*, 1(2), 2014.

[30] William R Leo. *Techniques for nuclear and particle physics experiments: a how-to approach*. Springer Science & Business Media, 2012.